

Cite this: *Soft Matter*, 2012, **8**, 8505

www.rsc.org/softmatter

PAPER

Effect of a non-volatile cosolvent on crack patterns induced by desiccation of a colloidal gel

F. Boulogne, L. Pauchard* and F. Giorgiutti-Dauphiné

Received 22nd March 2012, Accepted 7th June 2012

DOI: 10.1039/c2sm25663k

The consolidation of colloidal gels results in enormous stresses that are usually released by the formation of undesirable cracks. The capacity of a gel network to crack during drying depends on the existence and significance of a pressure gradient in the pore liquid; in addition it depends on the way the gel relaxes the resulting drying stresses. In this paper the effect of a binary mixture of solvents saturating the gel network on the crack patterns formation is investigated. Indeed, incorporation of a small quantity of non-volatile cosolvent, *i.e.* glycerol, inhibits drying-induced cracks; moreover addition of a concentration greater than 10% to a colloidal dispersion leads to a crack free coating under room conditions. Mass variation with time reveals that both evaporation rate and cracking time are not affected by glycerol, in the range of added glycerol contents studied. In addition measurements of mechanical properties show that the elastic modulus is reduced with glycerol content. The decrease of the number of cracks with the glycerol content is related to the flattening of the pressure gradient in the pore liquid. The mechanism is shown to be due to the combination of two processes: flow driven by the pressure gradient and diffusion mechanisms in accordance with Scherer's work (1989).

1. Introduction

Most coatings are made by depositing a volatile liquid that contains dispersed colloidal particles on a surface. The liquid is then evaporated until a dry film is obtained. Common examples in industrial fields are paints, protective coatings (anti-corrosion), and ceramic membranes.¹ Coatings are required to be homogeneous and smooth. Particularly they have to be free of heterogeneities possibly leading to cracking due to high stresses developing during the consolidation. In a liquid film, evaporation of the volatile solvent causes the solid particles to be confined to a smaller volume, until they come into direct contact with each other, and form a solid porous network, the so-called gel.² Then, further evaporation causes the liquid/air interface to curve into a set of menisci that join the particles. As a consequence the capillary forces exert extremely strong compressive stresses on the particle network. When the drying stress developed in the gel exceeds the strength of the material, undesirable effects occur such as the formation of various modes of cracking.^{3–6} As a consequence the stress in the gel is relaxed. Since numerous studies on cracks induced by drying of colloidal suspensions have been investigated for the last two decades, the stress development and the organization of colloidal particles in a drying film remain unclear. One of the main questions that still stands is: how can the stress be relaxed before cracks can form?

In addition, the development of stresses, hence of cracking, notably depends on the type of the particles (size⁷ and chemical composition^{4,8}) and mechanical properties of the gel formed,^{9,10} the substrate, the drying conditions (temperature,¹¹ relative humidity,¹² and air velocity¹³) and the film thickness.^{9,10,14} In particular the capacity of a gel network to crack during drying depends on the existence and significance of a pressure gradient in the pore liquid and the way the gel relaxes the induced drying stresses.

In the present work, we focus on the effect of cosolvent added to the colloidal dispersion on crack patterns induced by drying. Such an additive reveals crack-free drying when added to ceramic foams.¹⁵ Glycerol has been chosen as a cosolvent for interesting properties of high miscibility in water and low volatility, and because it exhibits a highly different intrinsic diffusion coefficient from that of water. Also glycerol is an element composing many essential fine arts products,¹⁶ due to its transparency properties and because it is used as a softener, avoiding creases and cracks. The crack patterns have been quantified as a function of the added glycerol content. The drying kinetics have been investigated by mass variation with time measurements. Also the mechanical properties of colloidal gels were measured by indentation testing as a function of the added cosolvent content. The experimental results can be explained by the combination of two processes occurring during the drying process: flow driven by the pressure gradient according to Darcy's law and a diffusion mechanism according to Fick's law.

CNRS, UMR 7608, Lab FAST, Bat 502, Campus Univ – F-91405, Orsay, France, EU. E-mail: pauchard@fast.u-psud.fr; Fax: +33 1 69 15 80 60; Tel: +33 1 69 15 80 49

2. Experimental

2.1. Materials and samples preparation

We used colloidal silica dispersion, Ludox HS-40, purchased from Sigma-Aldrich. The radius of the particles is 9 ± 2 nm, the density 2.36×10^3 kg m⁻³. The mass fraction of the initial dispersion was estimated to be $\phi_m = 40.5\%$ from a dry extract. Thus, we could deduce the particle volume fraction for this solution to be $\phi_v \approx 22\%$. Particles are polydisperse enough not to crystallize. In the absence of evaporation, the suspension is stable due to the competition between the attractive van der Waals forces and the electrostatic repulsion¹⁷ between particles (pH = 9.8).

Glycerol (purity: 99.0%, from Merck) was added to the aqueous dispersion as a cosolvent. This solvent exhibits high miscibility properties in water and low vapor pressure (2.2×10^{-4} mbar at 25 °C)¹⁸ compared to water (31.7 mbar). Thus, we assume glycerol as a non-volatile compound. The surface tension of pure glycerol is 62.5 mN m⁻¹ at 20 °C²⁹. The glycerol/water weight ratio was obtained using the following process: the resulting solution was filtered to 0.5 μm to eliminate eventual aggregates; the mass fraction is estimated from a dry extract at 140 °C. In order to keep the particle mass fraction constant for each sample, a given quantity of water is evaporated, then replaced by an equal mass of glycerol; the evaporation of water is achieved by stirring the aqueous dispersion at 35 °C in an Erlenmeyer flask. Finally, we checked the final pH of the solution.

We note κ to be the ratio between the mass of glycerol added and the mass of the resulting dispersion. Six solutions have been investigated: $\kappa = 1.1, 2.1, 3.1, 5.1, 7.2$ and 8.9% wt. This leads to glycerol fraction in solvent denoted by χ_i (the subscript stands for initial). In the range of glycerol content added, the solvent viscosity increases until 1.3 mPa s.

2.2. Drying geometry

Experiments are performed on films of fixed thickness. Also a small amount of the solution (initial weight $m_i = 0.52 \pm 0.02$ g) is deposited inside a circular container (diameter = 15 mm) whose bottom is a glass microscope slide carefully cleaned with ethanol and the lateral wall is a rigid rubber ring (Fig. 1(a)). The contact line of the solution is quenched at the upper edge of the circular wall and remains there during the whole experiment. In this geometry the layer dries at room temperature ($T = 23$ °C) under controlled relative humidity ($R_H \approx 50 \pm 2\%$). In this way, the desiccation takes place in the absence of convection in the vapor so that the evaporation is limited by diffusion of the solvent into the air. The drying kinetics is obtained using a scale (Sartorius)

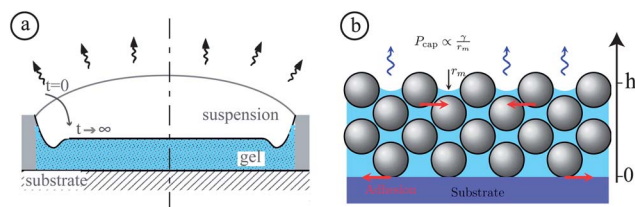


Fig. 1 (a) Experimental set-up (side view): during solvent loss the layer consolidates. (b) Sketch of the solid network saturated by solvent: curvature of the solvent/air menisci occurs at the evaporation surface during solvent loss and exerts an enormous stress on this network.

with an accuracy of 0.01 mg. When the gelled phase is formed, the layer exhibits an approximately constant thickness in a central region (Fig. 1(a)). In this region, covering about 70% of the total surface area, the evaporation is assumed to be uniform. A typical value of the thickness far from the border is $h \approx 0.7$ mm. The colloidal gel is transparent allowing us to observe easily the dynamics of crack patterns in the layer. Also the crack patterns formation is recorded using an interval timer with an AVT Marlin camera positioned on the top of the sample.

2.3. Measurements of the mechanical properties of the gel phase

To characterize the mechanical properties of the gelled layers relevant elastic modulus, E_p , indentation testing has been performed. This quantity has been determined using a CSM Instruments Micro Indentation Tester (MHT) with a four-sided pyramidal Vickers indenter. Indentation testing is a local method of mechanical investigation. The indenter, initially in contact with the surface of the gel, is driven in the material until a maximal 70 mN load with a loading speed 70 mN min⁻¹. The maximal force is held for 10 s. Then, the load is decreased until zero with the same speed. Fig. 5(a) shows a typical load/unload curve. The standard way of estimating the elastic modulus from the indentation load–displacement curve uses the initial slope of the unloading curve. Based on Sneddon's work,¹⁹ the following formula has been derived for the elastic modulus, E_p , to the unloading slope:^{20,21}

$$E_p = \frac{\sqrt{\pi}}{2} \frac{S}{\sqrt{A}}$$

In this equation, S is the slope of the unloading curve at the start of unloading and A is the projected area of contact between the indenter and the material at that point (inset in Fig. 5(a)). Note that the contact between the indenter and the gel is always chosen in a location where the layer adheres on the substrate. In the case of successive measurements of the elastic modulus with time, indentation testing was performed in the same adhering region to obtain comparable values as effectively as possible. Particularly, the difficulties of these measurements lie in gel films without glycerol addition exhibiting the smallest size of adhering regions. Indeed it has been observed that glycerol reduces the capacity of the gel to delaminate. In addition indentation testing applied to drying gelled layers has to be carefully analyzed since the system is not homogeneous in thickness and evolves with time. Also measurements of elastic moduli in gels by this method do not give absolute values but provide on the one hand a process of comparing mechanical properties of different materials and on the other hand a characterization of the time evolution of the mechanical properties of the system. Therefore measurements for the elastic modulus have been reproduced several times and performed on 2 or 3 samples; bars in Fig. 5(b) take into account the minimum and maximum measurements obtained.

3. Results

3.1. Drying

Once the layer is deposited in the circular trough, evaporation of the water takes place. The drying process of a colloidal dispersion

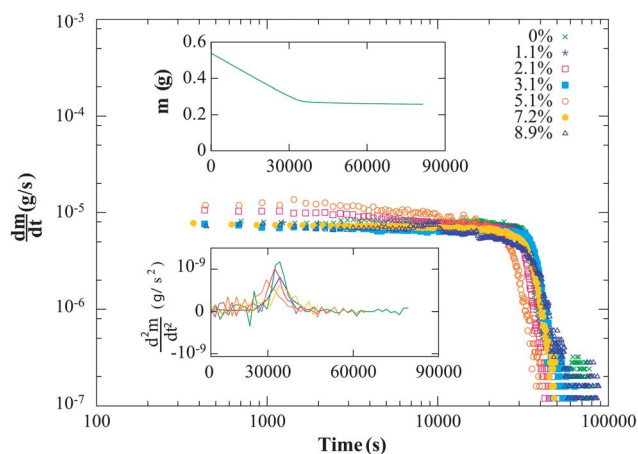


Fig. 2 Drying curves. Drying rate, $\frac{dm}{dt}$, for silica films for different additional glycerol concentrations, κ . The drying rate is calculated from the mass variation with time (upper inset). The variation $\frac{d^2m}{dt^2}$ with time evidences the transient time close to 32 000 s.

is usually separated into two stages that can be roughly distinguished by measuring mass, m , and drying rate, $\frac{dm}{dt}$, variations with time (Fig. 2).²² In the first regime (constant rate period) the evaporation rate is constant and evaporation is mainly controlled by the external conditions of relative humidity and temperature in the surroundings. During this stage, water removal concentrates the colloidal particles into a closed packed array: a porous network saturated with solvent. Due to geometry of the planar film, evaporation at the gel–air interface and adhesion at the gel–substrate interface result in the development of high stresses in the gel (Fig. 1(b)). Capillary pressure that is caused by the liquid menisci formed between the particles at the top of the packed region is responsible for the shrinkage of the porous network. The shrinkage of the gel at the gel–air interface is frustrated by the adhesion to the substrate. As a consequence tensile stresses progressively build up in the layer. Then a non-linear drying rate follows: the falling rate period, when liquid/air interfaces recede into the porous medium and when the drying process is limited by flow of liquid to the top layer through the porosity. The transient between the constant rate period and the falling rate period is highlighted in the lower inset in Fig. 2: it shows the drying rate derivative $\frac{d^2m}{dt^2}$. Under our experimental conditions we observe that the transient always occurs at $\sim 32\,000$ s in the studied κ range. Consequently the drying rate decreases as clearly shown in Fig. 2. Similar behaviors occur when glycerol content is added to the aqueous dispersion (Fig. 2).

3.2. Cracking

As the tensile stress reaches a threshold value, cracks appear in the film and invade the plane of the layer. First cracks appear at $t \in [24\,000, 27\,000]$ s after deposition of the layer on the substrate, without any correlation with the glycerol concentration or the initial mass disparity. Moreover the cracks invade the layer for only a few minutes. Thus the crack network develops during the initial stage of the drying process, in the constant rate period 2,

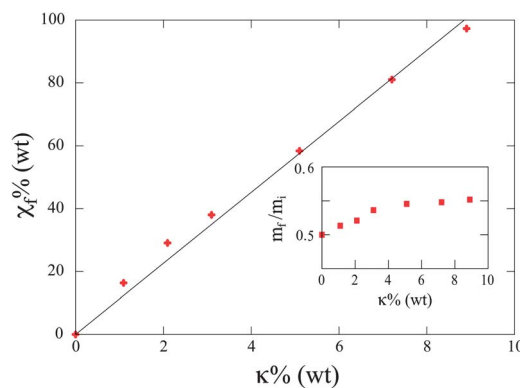


Fig. 3 Mass ratio of samples for different glycerol concentrations κ . The inset shows the final concentration of glycerol in the solvent wetting the porous medium as a function of κ . The solid line is a linear adjustment (slope = 11.3 ± 0.3).

and does not evolve afterwards. Plot in the inset in Fig. 3 shows the ratio, m_f/m_i , of the final (at $t = 60\,000$ s) and the initial mass of material on the glass plate (raw data). Furthermore, we know that silica particles contribute to 40% of the mass. Thus, the excess of mass is due to the solvent. As previously mentioned only water could evaporate and glycerol remains in the porous medium. Also we can calculate the mass fraction of glycerol χ_f composing the solvent when the mass variations with time do not evolve anymore ($t \approx 60\,000$ s):

$$\chi_f = 1 - \frac{m_f/m_i - 0.4 - \kappa}{m_f/m_i - 0.4} \quad (1)$$

We found that the higher the initial fraction κ , the higher the χ_f (see inset of Fig. 3), leading to a saturation of glycerol in the gel for $\kappa > 8.9 \pm 0.3\%$ in accordance with the fit.

Crack patterns are strongly modified by the presence of glycerol within the solvent. Indeed, in the case of a silica gel without additional glycerol, the successive formation of cracks results in the typical pattern shown in Fig. 4(a). This pattern is usually

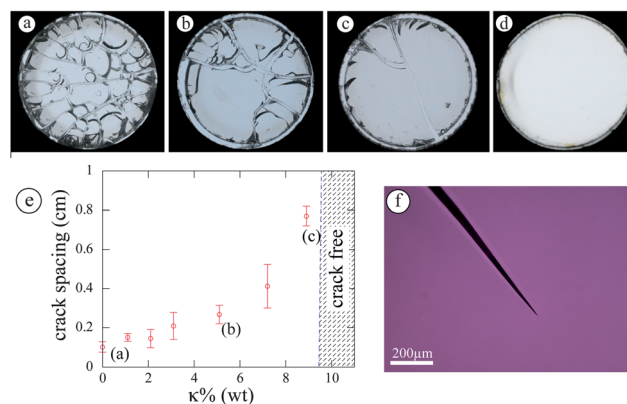


Fig. 4 Crack patterns after 16 hours in gelled layers when adding a second solvent to the system. (a) Without any additional glycerol. (b) $\kappa = 5.1\%$. (c) $\kappa = 8.9\%$. (d) $\kappa = 10.2\%$: the layer is crack-free at the mesoscopic scale. (e) Crack spacing plotted as a function of the concentration in glycerol (drying conditions $R_H = 50\%$ and $T = 23\text{ }^\circ\text{C}$; the initial weight deposited in each trough is the same). (f) Propagating crack tip in a gel with additional glycerol $\kappa = 8.9\%$.

continued by further crack generations: particularly a delamination process takes place when the gel detaches from the substrate.²³

Moreover final crack patterns are shown in Fig. 4(a)–(d) for increasing glycerol concentrations κ up to 10.2% under our experimental conditions. For each pattern, cracks still interconnect leading to a complete network: no broken network is observable suggesting that if crack nucleation is less favourable in the presence of additional glycerol, crack propagation is still not inhibited. The number of crack generated diminishes when the quantity of additional glycerol increases; this results in increasing the crack spacing as shown in Fig. 4(e). Fig. 4(f) shows a magnification of a typical crack tip propagating in a gel with glycerol content. The sharpness of this crack tip, also observed for every $\kappa \leq 9.5\%$, suggests that the gel still exhibits brittleness properties. In addition a buckle-driven delamination process, that usually takes place after the formation of a crack network, is inhibited by increasing additional glycerol concentration in the gel.

Above a threshold concentration of additional glycerol, the layer remains crack free (Fig. 4(d)): no crack forms because the gel could not reach the compaction (or the threshold stress) for which cracks propagate. It results in a flat gel film saturated in glycerol.

3.3. Gel consolidation

The macroscopic elastic response of the gel is characterized by indentation testing for various binary mixtures of solvents (Fig. 5). Based on the procedure depicted in Fig. 5(a), elastic moduli have been measured for gels of various glycerol contents. Each measurement has been obtained ~ 8 hours after the crack formation since the gel evolves slowly after this duration (Fig. 2). The measurements in Fig. 5(b) reveal that an increase of the quantity of glycerol in the gel results in a decrease of its elastic modulus. Since glycerol remains inside the porous medium, it could act as a wetting agent lowering the material stiffness.

The elastic modulus of silica gels has been measured as a function of time during the drying process; measurements started after crack propagation, $t > t_m$. These measurements are shown for the silica gel without any glycerol addition and for two glycerol contents in Fig. 5(c). In any cases, gel films clearly stiffen as they consolidate with time; for the silica gel without any glycerol addition, this process is more rapid than in the presence of glycerol content. Two factors could contribute to increase the modulus as a function of time: stiffening of the solid phase of the gel and reduction in the porosity.²⁴ Also the elastic modulus increases faster for gels having lower concentrations of glycerol.

4. Discussion

The capacity of a gel to crack during drying depends on the existence and significance of a pressure gradient in the pore liquid. Indeed the spatial variation in pressure causes a variation in contraction of the gel network.²⁵ This modifies the way the drying stresses are relaxed and consequently the cracks are formed. In the following the spatial variation in pressure in the liquid pore is characterized in gels saturated by binary mixtures of solvents during the first drying regime since cracks form during this stage. Particularly we have chosen to compare the pressure distribution for different glycerol contents at time

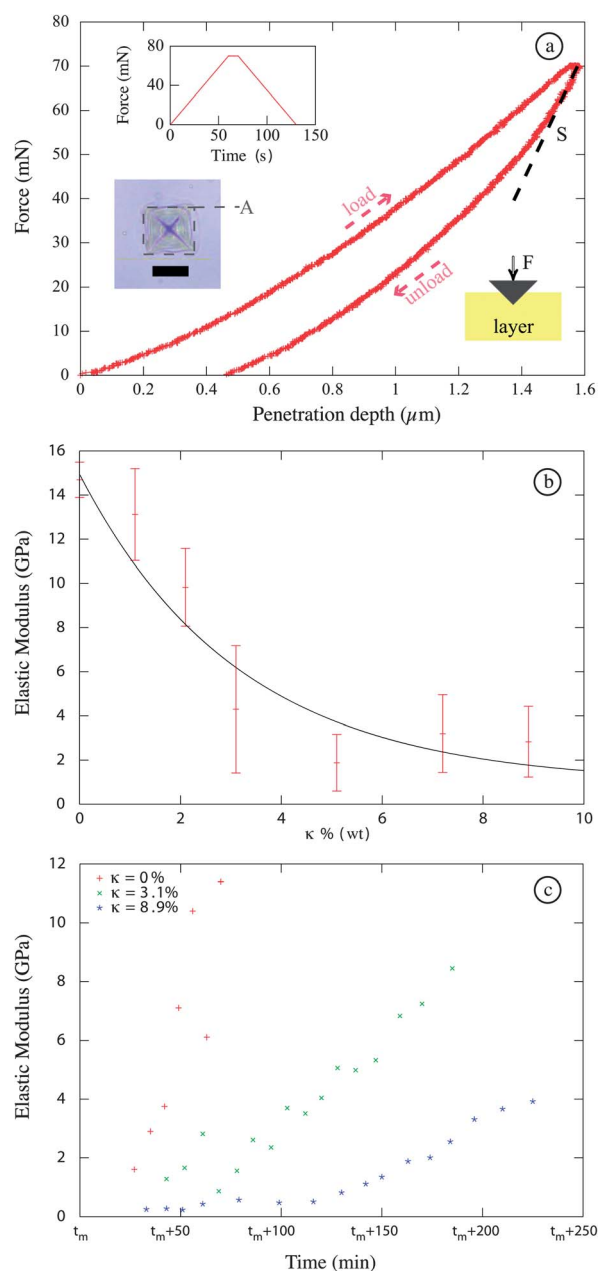


Fig. 5 Macroscopic elastic response of the gel obtained by indentation testing. (a) Loading/unloading curve: force applied on the tip versus indenter displacement (μm). Insets: variation of the applied force versus time; image of indentation print at the surface of the gel after a loading/unloading cycle observed using optical microscopy (maximum load: 70 mN, bar = 25 μm): the dashed square limits the projected area of contact, *A*. (b) Variation of the elastic modulus, E_p , for 7 glycerol–Ludox solutions. (c) Variation of the elastic modulus, E_p , as a function of time for Ludox HS-40 without glycerol addition ($\kappa = 0\%$) and for two different concentrations of glycerol ($\kappa = 3.1\%$, 8.9%). Measurements start after crack propagation, $t > t_m$.

$t_m = 25\,500$ s. At this moment, close to the typical cracking time of the gelled layers, gels can be considered as non-shrinking, that is, the gel network does not change with time;²⁵ pores contain the binary mixture of solvents and the liquid–air interfaces are already curved.

In drying gels, liquid usually moves through the network in response to a pressure gradient of liquid, $\frac{\partial P}{\partial z}$, accordingly to the Darcy law.² Also, in the case of a gel saturated with a single volatile solvent, the flux of evaporating liquid at the gel–air interface comes entirely from the flow of liquid. It is expressed as:

$$J_{\text{Darcy}} = \frac{k \partial P}{\eta \partial z} \quad (2)$$

where κ is the network permeability of the gel and η is the dynamic viscosity of the solvent in the pore; note that the pressure of the liquid pore is regarded as positive.

Let us now consider the incorporation of a soluble and non-volatile cosolvent, *i.e.* glycerol, to the aqueous dispersion. The drying process leads to a gel phase saturated by a binary mixture of water and glycerol. This results in a combination of the pressure flow component (2) and a diffusion mechanism.^{2,25,26} In that way, the diffusive flux for each component, i , is expressed in accordance with the Fick law:

$$J_{\text{Fick}}^i = -D_i \frac{\partial C_i}{\partial z} \quad (3)$$

where D_i is the intrinsic diffusion coefficient referred to in terms of the rate of transfer of component i across a fixed section. Note that P and C_i are time dependent.

The total fluid flux in the porous network combines the flow driven by the pressure gradient (2) and the diffusive flux (3). Also, the relative change in volume of liquid over time, \dot{V}_L/V_L , is due to the change in both local flow, $\partial_z J_{\text{Darcy}}$, and local diffusion flux, $\partial_z J_{\text{Fick}}$. As a result the following conservation equation can be written:²⁵

$$(1 - \rho) \frac{\dot{V}_L}{V_L} = -\partial_z J_{\text{Darcy}} - K \partial_z (J_{\text{Fick}}^1 + J_{\text{Fick}}^2) \quad (4)$$

where ρ is the relative density of the gel, K is the porosity of the gel, and J_{Fick}^i is the diffusive flux of component i , $i = 1$ for water and $i = 2$ for glycerol.

Since the change in the volume of liquid has to equal the change in pore volume, the following relation can be written in accordance with ref. 25:

$$(1 - \rho) \frac{\dot{V}_L}{V_L} = -\frac{1}{E_p} (\beta \dot{P} + (1 - \beta) \langle \dot{P} \rangle) \quad (5)$$

where β is a function of the Poisson ratio of the gel and \dot{P} is the time derivative of the pressure. Also the flux from the gel surface equals the rate of change in volume of the gel; this is expressed as $\langle \dot{P} \rangle = E_p \frac{V_E}{h}$ for a layer of thickness h according to ref. 25. Here the evaporation rate, V_E , determines the rate of volume loss by water evaporation.

By equating the right sides of expressions 4 and 5 and taking into account relations 2 and 3, we have:

$$\frac{\beta}{E_p} \frac{\partial P}{\partial t} + (1 - \beta) \frac{V_E}{h} = \frac{k}{\eta} \frac{\partial^2 P}{\partial z^2} + K(D_2 - D_1) \frac{\partial^2 C_1}{\partial z^2} \quad (6)$$

Eqn (6) reveals that the diffusion mechanism can become significant only when the intrinsic diffusion coefficients of cosolvents are sufficiently different from each other. Note that eqn (6) is only valid in the case of a solvent made of two

components: in the case of a pure solvent, the diffusive term (second term of the right side) disappears and the flow is only governed by the Darcy law. Applying eqn (6) to our system allows us to plot the pressure in a pore liquid of the gel for different glycerol contents. In that purpose the concentration of component 1 (water), C_1 , has to be incorporated in eqn (6); C_1 satisfies the diffusion equation using the boundary condition of constant flux at the evaporation surface, that is expressed as (ref. 26 p. 61): $-(\bar{C}_1 D_1 + (1 - \bar{C}_1) D_2) \frac{\partial C_1}{\partial z} \Big|_{z=h} = V_E$, where \bar{C}_1 is the mean concentration of water in the layer defined as:

$$\bar{C}_1(t_m) = \frac{1}{h} \int_0^h C_1(z, t_m) dz \text{ at time } t_m.$$

As a result an estimation of each quantity of eqn (6) from the experimental results is required. $\bar{C}_1(t_m)$ is precisely estimated from the inset in Fig. 3. In the first drying regime, V_E can be measured from the mass variation with time in Fig. 2 ($V_E \approx 4 \times 10^{-8} \text{ m s}^{-1}$). The values of the intrinsic coefficients are obtained from ref. 27: $\frac{D_2}{D_1} \approx 50$. The porosity K is roughly estimated to 0.40 for the random close-packed phase while $\beta = 1/2$ (ref. 25). We assume that the permeability of the gel remains constant during the crack formation; this quantity is estimated using the Carman–Kozeny relation ($k = 4.9 \times 10^{-19} \text{ m}^2$).²⁸ Finally the elastic moduli of gels composed with various glycerol contents have been estimated from experimental results shown in Fig. 5(b) and (c) extrapolating values a short time after cracking. Consequently, the concentration distribution C_1 and the pressure, P , are plotted along liquid pores at time t_m in Fig. 6 for different glycerol contents. The flattening of the pressure gradient when the concentration of glycerol increases is clearly observable and is mainly attributed to the diffusion mechanism. One should note that the reduction in the capillary forces near the surface should be of minor importance as the surface tension from one mixture to another varies only from $\sim 68 \text{ mN m}^{-1}$ to $\sim 72 \text{ mN m}^{-1}$.²⁹ These

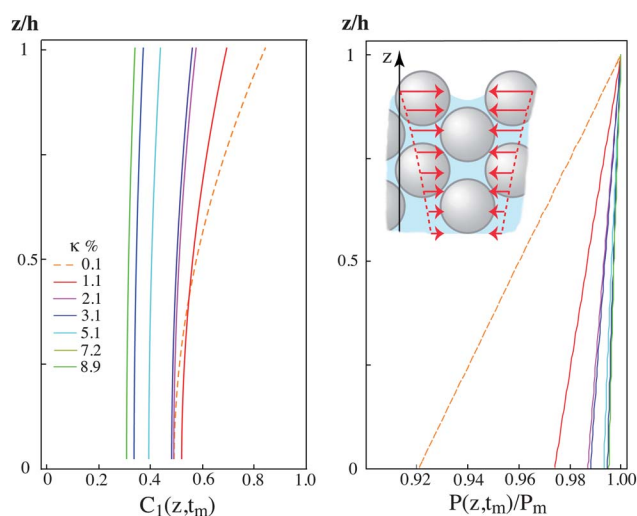


Fig. 6 Concentration distribution in water, C_1 , (left) and normalized pressure distribution, P/P_m , (right) along the pore liquid, for several initial glycerol contents, κ . These quantities are plotted at time t_m when the highest pressure value reaches P_m at the evaporation surface. Inset: sketch of the pressure gradient in the liquid pore.

results highlight the effect of the addition of a non-volatile solvent to the pressure in the liquid pore since diffusion can extract liquid from the interior and flatten the pressure gradient in the pore liquid. The pressure gradient causes a shrinkage that is transmitted in the hard particles network. In the present paper, the adhesion with the substrate is assumed to be a constant and to play a determinant role as responsible for the development of high stresses in the gel.^{30,31} Nevertheless the adhesion is seen as a necessary but not sufficient condition for cracking. Thus we eliminate cracking by modifying the pressure gradient and keeping constant the adhesion. The increase of glycerol content, through a diffusion process, will imply that the resulting drying stresses will be distributed more uniformly in the gel. Consequently, the stress concentration in the gel network is limited and the crack formation can be inhibited.

The effect of addition of glycerol content results in the flattening of the pressure gradient in the pore liquid due to a diffusion process as depicted by eqn (6), for a constant value of the elastic modulus. Moreover, the effect of addition of glycerol content results in the tendency of a decrease of the elastic modulus of the gel. As a consequence a decrease of the elastic modulus in eqn (6) leads to a flattening of the pressure gradient, and, in that sense, emphasizes the effect of diffusion.

5. Conclusion

The incorporation of a small percentage of non-volatile cosolvent modifies the way the drying stresses relax in a colloidal gel. Experimental data show that the drying rate and cracking time are not significantly modified by incorporation of the cosolvent. However the presence of non-volatile cosolvent decreases the stiffness of the gel at a given consolidation time and inhibits crack formation: incorporation of a concentration of glycerol greater than 10% in the colloidal dispersion results in a crack free drying gel. The mechanism is shown to be due to the combination of both flow driven by the pressure gradient and diffusion of one solvent into another; in this scenario the diffusion induced by evaporation causes a demixing effect of solvents. This results in a flattening of the pressure gradient in the pore liquid and consequently the distribution of the drying stresses is more uniform, limiting stress concentration in the gel network possibly because of cracking. Moreover, the effect of a cosolvent added to a silica dispersion on the crack pattern has been highlighted in the case of glucose. As in the case of glycerol, the presence of glucose in the gel film reveals an increase of the crack spacing. However, contrary to the case of glycerol, cracks are not completely inhibited above a threshold glucose content: the crack spacing tends to a maximum value (typically 0.45 cm under the same experimental conditions as for the glycerol cosolvent).

Finally, the effect of the flattening of the pressure gradient is surely not the only process leading to the diminution of the number of cracks in the gel film. Particularly chemical effects between glycerol and silanol groups covering the surfaces of silica particles could change the strength of the gel film. This process is suggested by aggregation rate measurements of silica

particles with polyols³² and would be of interest for further works applied to gel film cracks induced by desiccation with chemical additives.

Acknowledgements

The authors thank A. Aubertin, L. Auffray, C. Borget and R. Pidoux for technical supports. In addition we thank the referees for their valuable comments which improved the consistency of the manuscript.

References

- 1 N. Bassou and Y. Rharbi, *Langmuir*, 2009, **25**, 624–632.
- 2 C. J. Brinker and G. W. Scherer, *Sol-Gel Science: The Physics and Chemistry of Sol-Gel Processing*, Elsevier Science, 1990.
- 3 C. Allain and L. Limat, *Phys. Rev. Lett.*, 1995, **74**, 2981.
- 4 W. P. Lee and A. F. Routh, *Langmuir*, 2004, **20**, 9885–9888.
- 5 M. S. Tirumkudulu and W. B. Russel, *Langmuir*, 2005, **21**, 4938.
- 6 P. Xu, A. S. Mujumdar and B. Yu, *Drying Technol.*, 2009, **27**, 636–652.
- 7 E. R. Dufresne, E. I. Corwin, N. A. Greenblatt, J. Ashmore, D. Y. Wang, A. D. Dinsmore, J. X. Cheng, X. S. Xie, J. W. Hutchinson and D. A. Weitz, *Phys. Rev. Lett.*, 2003, **91**, 224501.
- 8 L. Pauchard, B. Abou and K. Sekimoto, *Langmuir*, 2009, **25**, 6672–6677.
- 9 A. Atkinson and R. M. Guppy, *J. Mater. Sci.*, 1991, **26**, 3869–3873.
- 10 A. Groisman and E. Kaplan, *Europhys. Lett.*, 1994, **25**, 415–420.
- 11 G. Gauthier, V. Lazarus and L. Pauchard, *Europhys. Lett.*, 2010, **89**, 26002–26006.
- 12 K. I. Dragnevski, A. F. Routh, M. W. Murray and A. M. Donald, *Langmuir*, 2010, **26**, 7747–7751.
- 13 L. Goehring, W. J. Clegg and A. F. Routh, *Langmuir*, 2010, **26**, 9269–9275.
- 14 H. Colina and S. Roux, *Eur. Phys. J. E: Soft Matter Biol. Phys.*, 2000, **1**, 189–194.
- 15 D. Fuks, G. E. Shter, M. Mann-Lahav and G. S. Grader, *J. Am. Ceram. Soc.*, 2010, 3632–3636.
- 16 R. J. Gettens and G. L. Stout, *Painting Materials: A Short Encyclopaedia*, Peter Smith Pub, 1966.
- 17 J. Laven and H. N. Stein, *J. Colloid Interface Sci.*, 2001, **238**, 8–15.
- 18 T. E. Daubert and R. P. Danner, *Physical and Thermodynamic Properties of Pure Chemicals: Data Compilation*, Hemisphere Publishing Corp New York, 4th edn, 1989.
- 19 I. N. Sneddon, *Int. J. Eng. Sci.*, 1965, **3**, 47–57.
- 20 W. Oliver and G. Pharr, *J. Mater. Res.*, 1965, **3**, 47–57.
- 21 J. Malzbender, J. M. J. den Toonder, A. R. Balkenende and G. de With, *Mater. Sci. Eng., R*, 1992, **7**, 1564–1583.
- 22 G. W. Scherer, *J. Non-Cryst. Solids*, 2002, **36**, 47–103.
- 23 L. Pauchard, *Europhys. Lett.*, 2006, **74**, 188–194.
- 24 G. W. Scherer, *J. Non-Cryst. Solids*, 1989, **109**, 183–190.
- 25 G. W. Scherer, *J. Non-Cryst. Solids*, 1989, **107**, 135–148.
- 26 J. Crank, *The Mathematics of Diffusion*, Clarendon Press, 2nd edn, 1975.
- 27 G. D'Errico, O. Ortona, F. Capuano and V. Vitagliano, *J. Chem. Eng. Data*, 2004, **49**, 1665–1670.
- 28 F. Dullien, *Porous Media, Second Edition: Fluid Transport and Pore Structure*, Academic Press, 1991.
- 29 D. Lide, *CRC Handbook of Chemistry and Physics*, CRC Press/Taylor and Francis, 89th edn, 2008.
- 30 R. C. Chiu and M. J. Cima, *J. Am. Ceram. Soc.*, 1993, **76**, 2769–2777.
- 31 R. C. Chiu, T. J. Garino and M. J. Cima, *J. Am. Ceram. Soc.*, 1993, **76**, 2257–2264.
- 32 G. L. Gulley and J. E. Martin, *J. Colloid Interface Sci.*, 2001, **241**, 340–345.